Geophys. J. Int. (2004) **159,** 212–222 doi: 10.1111/j.1365-246X.2004.02365.x

Instability of a periodic system of faults

Michel Campillo,[1] Cristian Dascalu[2] and Ioan R. Ionescu[3]

[1]*Laboratoire de Géophysique Interne,* PO Box 53X, 38041 *Grenoble Cedex, France. E-mail: michel.campillo@obs.ujf-grenoble.fr*
[2]*Laboratoire* 3S, PO Box 53X, 38041 *Grenoble Cedex, France. E-mail: cristiandascalu@hotmail.com*
[3]*Laboratoire de Mathématiques,* 73376 *Le Bourget-du-Lac Cedex, France. E-mail: ionescu@univ-savoie.fr*

Accepted 2004 May 20. Received 2004 May 20; in original form 2002 September 9

SUMMARY

To investigate the effect of heterogeneity of resistance on a fault, we present an analysis of the behaviour of a canonical model, namely a periodic system of coplanar faults that can slip under a slip-weakening friction law. The friction on the sliding patches is characterized by a weakening rate α. We present a stability analysis based on the decomposition of the solution on a set of eigenfunctions of increasing periodicities that are multiples of the natural period of the system. We discuss the structure of the discrete spectrum of the static solution. For a given geometry, we show that there exists a transition value α_0 of weakening rate defining two distinct regimes. When α is smaller than α_0, the system is stable, while when α is larger than α_0, unstable modes with exponential growth are present. This stability limit can be regarded as a non-local criterion of sliding. A somehow surprising result is the fact that a system with infinite extension can exhibit a stable behaviour. Specifically, we show that even a fault with weakening almost everywhere can be stable. An infinite homogeneous fault, on the contrary, is always unstable as soon as weakening is assumed. To understand this apparent paradox, we refer to the concept of the effective friction law, which describes the large scale behaviour of the fault system, and more precisely here to the effective weakening rate. The results presented here indicate that the effective friction law of a periodic fault system with weakening on the sliding parts can be either a weakening or strengthening law depending on the geometry of the surface of sliding.

Key words: earthquake-source mechanism, eigentheory, elastic wave theory, fault slip, spectral analysis.

1 INTRODUCTION

A key issue for the construction of a fault model is the applicability of laboratory results on friction parameters to the scale of actual faults. In the context of the slip-weakening model with constant stress drop, the critical slip of weakening D_c (Ida 1972; Palmer & Rice 1973) governs the dynamic evolution (Andrews 1985; Matsu'ura *et al.* 1992). It is noticeable that the values of D_c used to model actual earthquake records (Ide & Takeo 1997; Peyrat *et al.* 2001; Aochi & Fukuyama 2002) are very different from the ones inferred from dynamic laboratory experiments. Indeed this critical slip must not be confused with the critical slip involved in rate and state laws (Ruina 1983; Dieterich 1986) as discussed in Guatteri *et al.* (2001). The slip-weakening model consists of imposing as a boundary condition the relation between displacement and stress observed during dynamic laboratory experiments of initiation and slip (Ohnaka 1996). This is not a valid approach for long-term evolution of the fault but, during the period corresponding to the experiments, it is the mechanical expression of the physical evolution of the slipping surface.

The friction properties are likely heterogeneous on the fault, particularly with the presence of barriers. By the term barrier, we denote a patch on the fault plane where no slip occurs. This concept cannot be applied for the evolution of the fault at the geological timescale but it has been shown to be useful and relevant in the description of fault heterogeneity during an earthquake (Papageorgiou & Aki 1983a,b). The nature of the barriers is beyond the scope of this paper. We consider here that the heterogeneity can be described by a single local parameter, namely the static friction threshold. Because of the heterogeneity the large-scale behaviour is controlled both by the friction at the elementary scale, that can be identified with the laboratory scale, and by the fine geometry of the distribution of resistance on the fault. Campillo *et al.* (2001) and Voisin *et al.* (2002) proposed a simple approach of rescaling based on the spectral solution of the evolution problem of shear instability. They interpret the behaviour of a segmented fault in terms of an effective friction acting uniformly on a homogeneous fault. Furthermore, Perfettini *et al.* (2003) proposed a simple scaling of the effective weakening rate of a heterogeneous fault. We study here a canonical problem for understanding the scaling of friction law: the case of a periodic system of antiplane finite faults. We specifically address the problem of

its limit of stability. We investigate the structure of the spectrum of the static solution. By analogy with the case of an infinite homogeneous fault, we interpret the existence of a stability limit for the heterogeneous periodic system in terms of an effective weakening rate at the onset of initiation.

2 PHYSICAL MODEL

Consider the antiplane shearing of a homogeneous linear elastic space containing a system of faults Γ_f, situated in the plane $y = 0$ and on which a slip-dependent friction law is supposed. We assume that the displacement field is zero in directions Ox, Oy and that u_z does not depend on z. The displacement is therefore simply denoted by $w(t, x, y)$. The elastic medium has the shear rigidity G, the density ρ and the shear velocity $c = \sqrt{G/\rho}$. The non-vanishing shear stress components are $\sigma_{zx} = \tau_x^\infty + G\frac{\partial w}{\partial x}(t, x, y)$, $\sigma_{zy} = \tau_y^\infty + G\frac{\partial w}{\partial y}(t, x, y)$ and the normal stress on the fault plane is $\sigma_{yy} = -S$ ($S > 0$).

The equation of motion is:

$$\frac{\partial^2 w}{\partial t^2}(t, x, y) = c^2 \Delta w(t, x, y), \tag{1}$$

for $t > 0$, $y \neq 0$. The boundary conditions on fault plane Γ_f are:

$$\sigma_{zy}(t, x, 0+) = \sigma_{zy}(t, x, 0-), \tag{2}$$

$$\sigma_{zy}(t, x, 0) = \mu[x, \delta w(t, x)] S \operatorname{sign}\left[\frac{\partial \delta w}{\partial t}(t, x)\right] \quad \text{if} \quad \frac{\partial \delta w}{\partial t}(t, x) \neq 0, \tag{3}$$

$$|\sigma_{zy}(t, x, 0)| \leq \mu[\delta w(t, x)] S \quad \text{if} \quad \frac{\partial \delta w}{\partial t}(t, x) = 0, \tag{4}$$

where $\delta w(t, x) = w(t, x, 0+) - w(t, x, 0-)$ is the relative slip.

The initial conditions are denoted by w_0 and w_1, i.e.:

$$w(0, x, y) = w_0(x, y), \frac{\partial w}{\partial t}(0, x, y) = w_1(x, y). \tag{5}$$

Because the direction of slip is given by the applied stress $\tau_y^\infty > 0$, let us assume in the following that the slip δw and the slip rate $\partial_t \delta w$ are non-negative. The friction law is assumed to be homogeneous on the slipping patches having the form of a piecewise linear function:

$$\mu(x, u) = \mu_s - \frac{\mu_s - \mu_d}{2L_c} u \text{ if } u \leq 2L_c, \mu(x, u) = \mu_d \quad \text{if} \quad u > 2L_c, \tag{6}$$

where u is the relative slip, μ_s and μ_d ($\mu_s > \mu_d$) are the static and dynamic friction coefficients and L_c is the critical slip. This piecewise linear function is a reasonable approximation of the experimental observations reported by Ohnaka *et al.* (1987).

Because our intention is to study the evolution of the elastic system near an unstable equilibrium position, we shall suppose that $\tau_y^\infty = S\mu_s$. We remark that taking w as a constant satisfies eqs (1–4), hence $w \equiv 0$ is an equilibrium position. Because we deal with the evolution of one initial pulse, we may put (for symmetry reasons) $w(t, x, y) = -w(t, x, -y)$, hence we consider only one half-space $y > 0$ in eqs (1) and (5). With these assumptions eqs (2–4) become:

$$w(t, x, 0+) = 0 \quad x \notin \Gamma_f, \tag{7}$$

$$\frac{\partial w}{\partial y}(t, x, 0+) = -\alpha w(t, x, 0+) \quad \text{if} \quad w(t, x, 0+) \leq L_c, \quad x \in \Gamma_f, \tag{8}$$

$$\frac{\partial w}{\partial y}(t, x, 0+) = -\alpha L_c \quad \text{if} \quad w(t, x, 0+) > L_c, \quad x \in \Gamma_f, \tag{9}$$

where α is a parameter that has the dimension of a wavenumber (m^{-1}) and that will play an important role in our further analysis. α is given by:

$$\alpha = \frac{(\mu_s - \mu_d)S}{GL_c}.$$

With the slip heterogeneity implied by the unbreakable barriers (eq. 7), the solution exhibits stress singularities located at the edges of the barriers. We have assumed an infinite resistance of the barriers and therefore we do not consider any evolution of their geometry in the mathematical treatment of the problem. We shall return to this point in the final discussion.

Because we assume that the initial perturbation (w_0, w_1) of the equilibrium ($w \equiv 0$) is small, we have $w(t, x, 0+) \leq L_c$ for $t \in [0, T_c]$ for all x, where T_c is a critical time for which the slip on the fault reaches the critical value L_c at least at one point, i.e. $\sup_{x \in R} w(T_c, x, 0+) = L_c$. Hence for a first period $[0, T_c]$ we deal with a linear initial and boundary value problem in eqs (1), (5) and (7). Our aim is to analyse the evolution of the perturbation during this initial phase.

Let us consider the eigenvalue problem associated with eqs (1), (5) and (7): find a bounded eigenfunction Φ: $R \times R_+ \to R$ and the eigenvalue λ^2 such that

$$\nabla^2 \Phi(x, y) = \lambda^2 \Phi(x, y), y > 0, \tag{10}$$

$$\frac{\partial \Phi}{\partial y}(x, 0+) = -\alpha \Phi(x, 0+), \quad x \in \Gamma_f, \tag{11}$$

$$\Phi(x, 0+) = 0, \quad x \notin \Gamma_f. \tag{12}$$

The eigenvalues λ^2 are functions of the parameter α, i.e. $\lambda^2 = \lambda^2(\alpha)$. It is important to obtain a simple condition on α to determine the positiveness of the eigenvalues λ^2, representing an unstable behaviour for the solution of the dynamic problem. Let us now make a remark that is extremely important for the analysis presented in this paper. The domain of existence of unstable solutions (i.e. $\lambda^2 > 0$) is limited by the critical values of the parameter α, for which $\lambda^2(\alpha) = 0$. For this reason we rewrite eqs (10–12) into a new eigenvalue problem corresponding to the static case (i.e. $\lambda^2 = 0$), in which the unknowns are α (such that $\alpha \geq 0$) and the eigenfunction $\varphi : R \times R_+ \to R$:

$$\nabla^2 \varphi(x, y) = 0, y > 0, \tag{13}$$

$$\frac{\partial \varphi}{\partial y}(x, 0+) = -\alpha \varphi(x, 0+), \quad x \in \Gamma_f, \tag{14}$$

$$\varphi(x, 0+) = 0, \quad x \notin \Gamma_f. \tag{15}$$

The solutions of this static eigenvalue problem are the stability limits in α of the different modes in a given geometry.

Let us be reminded that we impose a positivity constraint on the solution $w(t, x, 0^+)$ on the fault Γ_f. This condition has not to be imposed on each eigenfunction. Having in mind the spectral expansion of the solution in terms of eigenfunctions, only their linear combination, with coefficients depending on the particular initial conditions, must comply with this requirement. Because the solution is dominated by the first eigenfunction, which has always the largest coefficient of exponential growth with time, the positivity constraint has to be applied to this particular eigenfunction. Although not a mathematically sufficient condition, we require that the first eigenfunction has the same sign everywhere on the fault in order for the eigenvalue problem to have a physical interpretation. This is always the case for a coplanar system of faults. If the faults are not coplanar, this condition is no longer satisfied, that is the above eigenvalue problem has no physical significance and a non-linear eigenvalue problem must be considered (Ionescu & Wolf 2004; Wolf *et al.* 2004). This difficulty arises with the effect of stress shadowing, which does not exist for the coplanar segments considered here.

3 SPECTRAL SOLUTION

In this section, we use explicitly the periodic character of the system of faults Γ_f. Let $P > 0$ be the geometrical period and let $[a, b]$ be the elementary fault ($0 < a < b < P$) of length $2L = b - a < P$ (see Fig. 1). The slipping part of the fault is given by

$$\Gamma_f = \cup_{k \in \mathbb{Z}} [a + kP, b + kP]. \tag{16}$$

As a result of the periodicity of the problem, we expect a periodic behaviour for the eigenfunction $x \to \varphi(x, y)$. To better point out this periodicity of the solutions, let us distinguish between the geometrical period of the fault system and the physical period of the corresponding spectral solution (Fig. 1).

Specifically, for a period P, we shall look for eigenfunctions $\varphi^m(x, y)$ of the static eigenproblem of periodicity mP with $m = 1, 2, \ldots$. That is, we are looking for $\varphi^m : \Omega \to R$ and α^m solution of

$$\nabla^2 \varphi^m(x, y) = 0, \quad y > 0, \tag{17}$$

$$\varphi^m(x + mP, y) = \varphi^m(x, y), \tag{18}$$

$$\frac{\partial \varphi^m}{\partial y}(x, 0+) = -\alpha^m \varphi^m(x, 0+), \quad x \in \Gamma_f, \tag{19}$$

$$\varphi^m(x, 0+) = 0, \quad x \notin \Gamma_f. \tag{20}$$

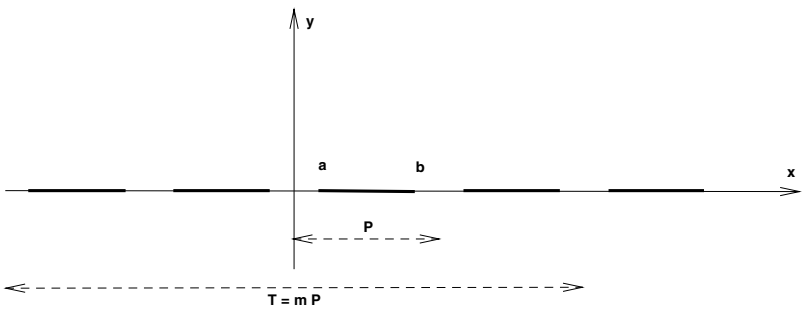

Figure 1. The geometry of the periodic fault. P is the geometrical period and $T = mP$ the physical period.

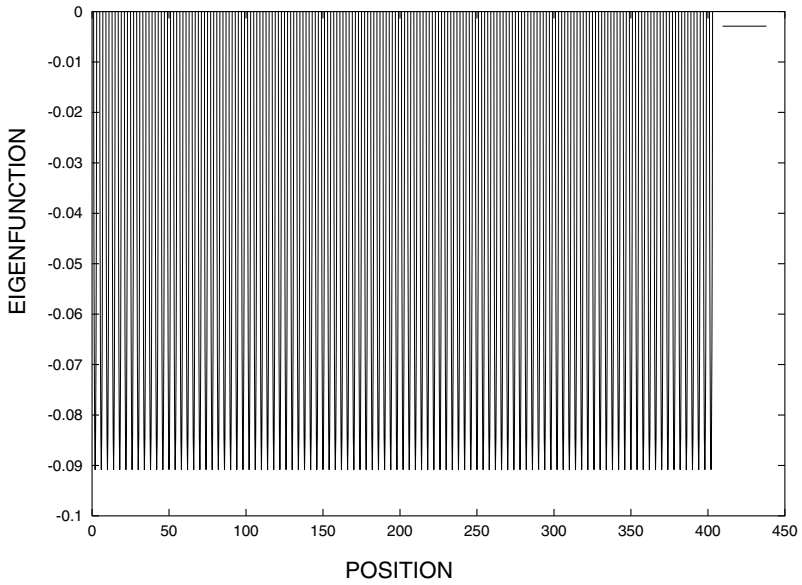

Figure 2. The eigenfunction $\varphi_0^{100}(x, 0)$ versus the fault line axis x. Note that its periodicity is P, i.e. $\varphi_0^{100}(x, 0) = \varphi_0^1(x, 0)$.

To solve this problem, we use the technique described in Appendix A with the parameter set: $T = mP$, $N = m$, $a_i = a + i\,P$ and $b_i = b + i\,P$, with $i = \overline{1, m}$. As it follows from Ionescu *et al.* (2002) for all m, the eigenvalues are an unbounded, non-decreasing sequence $(\alpha_n^m)_{n\geq 1}$, i.e.

$$0 < \alpha_0^m \leq \alpha_1^m \leq \ldots \leq \alpha_n^m \leq \ldots, \qquad \lim_{n\to\infty} \alpha_n^m = +\infty. \tag{21}$$

3.1 Stability analysis

The system in eqs (17–19) was numerically solved for different values of m using the method described in Appendix A for $P = 4L$ and $[a, b] = [L, 3L]$, where L is a characteristic length. The first eigenvalue α_0^1 of the elementary periodicity P is also the first eigenvalue of periodicity mP for all m, simply denoted by α_0. We denote by φ_0 the associated eigenfunction, i.e.

$$\alpha_0^m = \alpha_0^1 = \alpha_0, \quad \text{for all} \quad m \geq 1,$$

$$\varphi_0^m(x, y) = \varphi_0^1(x, y) = \varphi_0(x, y), \quad \text{for all} \quad m \geq 1.$$

In order to illustrate this fact we have plotted in Fig. 2 $\varphi_0^{100}(x, 0)$ computed for $P = 4L$, which is actually a periodic function of the same period P and not only $100P$ as could be expected for the first eigenvalue. The unexpected property that α_0 is the first eigenvalue whatever the periodicity seems to be a general feature that we observed for all the cases we have considered in our computations. Because we are not able to prove it from a mathematical point of view, we conjecture that for a geometric periodicity P, in the set of solutions of period mP, the eigenfunction associated with the first (the smallest) eigenvalue is a function of period P.

The first eigenvalue α_0 represents the threshold of instability, that is

$$w \equiv 0 \quad \text{is unstable when} \quad \alpha > \alpha_0. \tag{22}$$

The positivity of α_0 in eq. (22), shows the possible existence of a stable periodic system of faults under slip-weakening friction.

Let us analyse now the influence of the length of the barrier on the stability limit α_0. For this, we consider a fault of length $2L$ and the non-dimensional parameter $r \in [0, 1]$ given by

$$r = \frac{2L}{P}.$$

In Fig. 3, we have plotted the computed non-dimensional threshold $\alpha_0\, L$ versus the geometrical parameter r. As expected, the system is more unstable when the barriers become shorter. Two geometric limit cases have to be noted. The first one corresponds to r close to zero. In this case, the faults are far away from each other and the stability limit is the same as for a single fault system obtained by Dascalu *et al.* (2000) and Uenishi & Rice (2003), i.e.

$$\alpha_0 L = \beta_0^* = 1.15777\ldots, \qquad \text{for} \quad r = 0.$$

The second limit case corresponds to the geometry of the periodic system of faults in which the barriers reduce to points. Computation performed for $P = 2L$ and $[a, b] = [0, 2L]$, with barriers at points $2kL$, $k \in \mathbb{Z}$, lead to a critical limit of stability

$$\alpha_0 L = 0.1532293\ldots, \qquad \text{for} \quad r = 1.$$

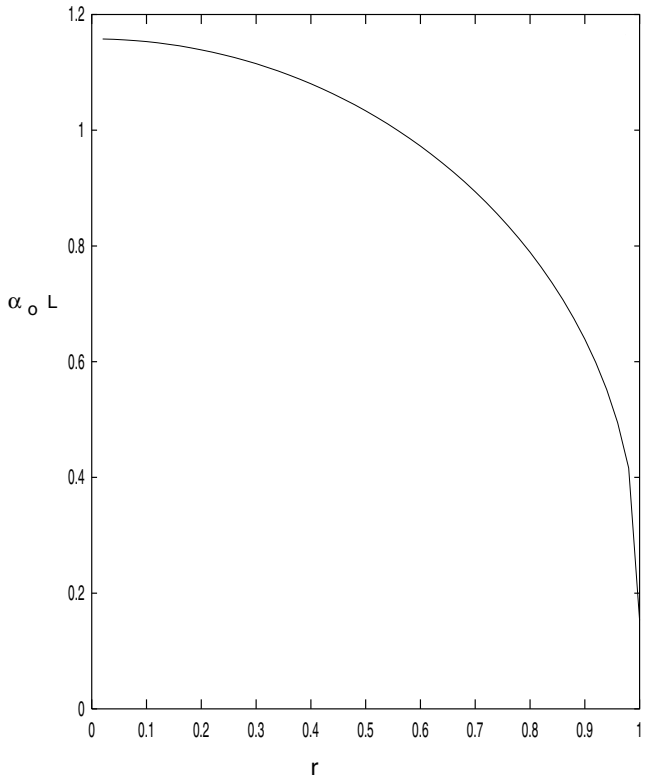

Figure 3. The computed non-dimensional threshold of stability $\alpha_0 L$ versus the geometrical parameter r.

Table 1. The eigenvalue α_1^m for different values of m.

	$m = 1$	$m = 2$	$m = 10$	$m = 20$	$m = 100$
$L\alpha_1^m$	2.764167	1.22235793	1.098298515	1.06730381	1.04040256

The non-vanishing of this limit shows that even for arbitrary small barriers there still exists a positive threshold of stability. This non-trivial result indicates that regions of resistance with very limited extent can play a major part in the global behaviour of a fault. Even when the surface of the barriers on the fault tends to zero, their existence can prevent the onset of an instability.

3.2 Description of the spectrum

We summarize here the principal facts deduced from numerical results obtained by solving eqs (17–19) with the method described in Appendix A. Considering $P = 4L$ and $[a, b] = [L, 3L]$, we found

$\alpha_0 = 1.03349339$

and the values of $\alpha_1^m L$, which are presented in Table 1.

From the results in Table 1 one can conjecture that

$$\alpha_1^m \to \alpha_0 \quad \text{for} \quad m \to \infty. \tag{23}$$

This property was verified in different numerical tests. This shows that for $\alpha > \alpha_0$, arbitrarily close to α_0, an infinite set of eigenfunctions Φ_1^m of the dynamic problem in eqs (10–12) have an unstable behaviour $[\lambda^2(\alpha) > 0]$.

We plotted in Fig. 4 the shape of the eigenfunction φ_1^{100}. We remark that the period is now 100 P, in contrast to φ_0^{100} of period P. A sinusoidal shape can be observed for the envelope of φ_1^{100}. One can note that the sign of the function changes. Therefore this function alone cannot comply with the positivity constraint. The positivity of the global solution is provided by the summation of the modes and predominantly by the first mode.

The details of the spectral structure of the solution are given in Appendix B. Simple properties of the distribution of the eigenvalues are shown. The relative positions of the eigenvalues can be interpreted by considering the different modes of interactions between neighboring segments as illustrated by the eigenfunctions on the fault.

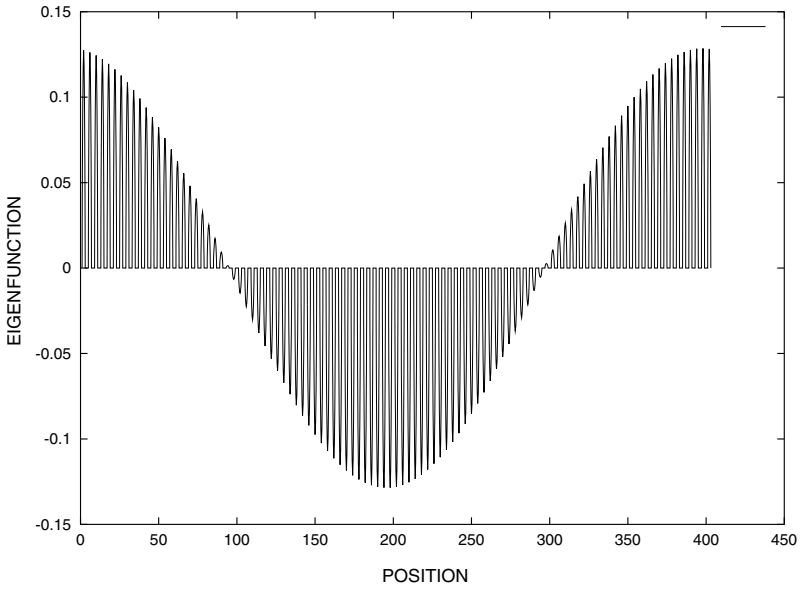

Figure 4. The computed eigenfunction $\varphi_1^{100}(x, 0)$ versus the fault line axis x. Note the sinusoidal shape of the envelope.

4 ANALOGY WITH THE INFINITE HOMOGENEOUS FAULT

We recall here the spectral analysis given by Campillo & Ionescu (1997), in the case of an infinite homogeneous fault, i.e. Γ_f is the whole x-axis. The same problem was studied with a different method by Knopoff *et al.* (2000) and Ampuero *et al.* (2002).

We have to solve the following eigenvalue problem: find a bounded eigenfunction Φ: $R \times R_+ \to R$ and the eigenvalue λ such that

$$\nabla^2\Phi(x, y) = \lambda^2\Phi(x, y), \quad y > 0, \tag{24}$$

$$\frac{\partial\Phi}{\partial y}(x, 0+) = -\alpha\Phi(x, 0+). \tag{25}$$

Using the separation of the variables, we found that $\lambda^2 \leq \alpha^2$ and that two types of eigenfunctions exist. The first one is given by:

$$\Phi^{\mathrm{I}}_{\lambda}(x, y) = C^{\mathrm{I}}_{\lambda} \exp(-\alpha y + ix\sqrt{\alpha^2 - \lambda^2}), \tag{26}$$

for all $\lambda \leq \alpha^2$. This expression contains a unique exponential dependance on y. Furthermore, a second type of eigenfunction is obtained for $\lambda^2 < 0$. In this case, for each λ^2, there exists a family of eigenfunctions given by:

$$\Phi^{\mathrm{II}}_{\lambda\beta}(x, y) = C^{\mathrm{II}}_{\lambda\beta} \exp(ix\sqrt{\beta - \lambda^2}) \left[\cos(y\sqrt{-\beta}) - \frac{\alpha}{\sqrt{-\beta}} \sin(y\sqrt{-\beta})\right], \tag{27}$$

for all β such that $\lambda^2 \leq \beta < 0$. This expression contains wave-type terms. In the expressions of the eigenfunctions, C^{I}_{λ}, $C^{\mathrm{II}}_{\lambda\beta}$ are normalization complex constants. Bearing in mind the above spectral computations, one can give a generic form of the solution for eqs (1), (5) and (7) as follows:

$$\begin{aligned} w(t, x, y) = &\int_0^{\alpha^2} \left[ch(\lambda ct)W^{\mathrm{I}}_0(\lambda) + \frac{sh(\lambda ct)}{\lambda c} W^{\mathrm{I}}_1(\lambda)\right] \Phi^{\mathrm{I}}_{\lambda}(x, y)\, d\lambda \\ &+ \int_{-\infty}^{0} \left[\cos(\lambda ct)W^{\mathrm{I}}_0(\lambda) + \frac{\sin(\lambda ct)}{\lambda c} W^{\mathrm{I}}_1(\lambda)\right] \Phi^{\mathrm{I}}_{\lambda}(x, y)\, d\lambda \\ &+ \int_{-\infty}^{0} \left\{\int_{\lambda^2}^{0} \left[\cos(\lambda ct)W^{\mathrm{II}}_0(\lambda, \beta) + \frac{\sin(\lambda ct)}{\lambda c} W^{\mathrm{II}}_1(\lambda, \beta)\right] \Phi^{\mathrm{II}}_{\lambda\beta}(x, y) d\beta\right\} d\lambda, \end{aligned} \tag{28}$$

where $W^{\mathrm{I}}_0(\lambda)$, $W^{\mathrm{I}}_1(\lambda)$, $W^{\mathrm{II}}_0(\lambda, \beta)$, $W^{\mathrm{II}}_1(\lambda, \beta)$ are deduced from the initial data w_0, w_1. This is a complete solution of the problem, having all the properties of the wave equation, including causality.

The part of the solution associated with positive eigenvalues, that is the first term in eq. (28), grows exponentially with time. Hence, after a while, this part will completely dominate the other part, which has a wave-type evolution. This is why we put $w = w^{\mathrm{d}} + w^{\mathrm{w}}$, where w^{d} is the dominant part and w^{w} is the wave part. As shown in Campillo & Ionescu (1997), the dominant part has a simple expression:

$$\begin{aligned} w^{\mathrm{d}}(t, x, y) = \frac{\alpha}{\pi} e^{-\alpha y} \Bigg\{ &\int_{-\alpha}^{\alpha} \int_0^{\infty} \int_{-\infty}^{\infty} e^{-\alpha s + i\lambda(x-u)} \Bigg[ch(ct\sqrt{\alpha^2 - \lambda^2})w_0(u, s) \\ &+ \frac{sh(ct\sqrt{\alpha^2 - \lambda^2})}{c\sqrt{\alpha^2 - \lambda^2}} w_1(u, s)\Bigg] du\, ds\, d\lambda\Bigg\}. \end{aligned} \tag{29}$$

According to this expression, the infinite homogeneous fault is unstable for any weakening rate ($\alpha > 0$). We can therefore define a stability limit as $\alpha = 0$ with reference to our previous analysis of the periodic fault. This is a drastic difference to the case of the periodic fault for which a non-zero limit of stability exists, even in the limit when the width of the barriers tends to zero.

To compare the behaviour of homogeneous and periodically heterogeneous infinite faults, we refer to the concept of effective friction as introduced by Campillo *et al.* (2001). The effective friction law is the law which, when imposed on a homogeneous fault, would produce the same average behaviour as that of the actual heterogeneous fault. It is a homogenized form of the friction. The validity of the approach has been demonstrated in the unstable regime and interpreted as a spectral equivalence of the homogeneous and heterogeneous problems Voisin *et al.* (2002).

To draw an analogy between the periodic and infinite cases is somehow delicate because their evolutions are characterized by continuous and discrete spectra, respectively. Nevertheless, the solution is governed by the largest eigenvalue and this eigenvalue belongs to the mode that defines the stability domain. In this sense, the static analysis gives important qualitative indications of the dynamic behaviour. The study of the structure of the spectrum of the periodic fault shows that the eigenvalues are accumulated in infinite number around the stability limit. This suggests a spectrum that is dense around the largest eigenvalue. From this observation, it seems legitimate to consider a spectral equivalence between the periodic and infinite problems, even considering that, in the case of the periodic fault, the only results available so far are the static eigenvalue solutions.

Let us consider a periodic fault with a given geometry. If the weakening on the sliding patches is larger than α_0, it is an unstable system. Its evolution is dominated by the most unstable mode, that is the first eigenfunction, which has a periodicity P and whose envelope is a constant (Fig. 1). If we consider the envelope as an average behaviour of the slip, we see here a property that is exhibited by the infinite fault, that the largest wavelengths are associated with the most rapid growth.

The existence of a limit of stability for the periodic fault is puzzling. It indicates that it is not always possible to define an effective weakening, because a homogenized infinite fault would always be unstable if subjected to a weakening friction. We understand this fact by taking into account the response of the unbreakable barriers. They offer an elastic resistance that counterbalances the weakening on the sliding patches. The resulting effect is producing the effective weakening. It results in the fact that the introduction of small resistant zones changes drastically the behaviour of the fault and decreases the effective weakening as illustrated numerically in Campillo *et al.* (2001). In the case of the periodic fault and depending on the geometry and the local weakening, this concurrence between weakening and elastic response results either in an average weakening, corresponding to the unstable regime, or in an average strengthening that is the stable regime of the infinite periodic fault. The effective friction law of a periodic fault can be therefore a weakening or strengthening friction.

5 SUMMARY AND DISCUSSION

We use the canonical configuration of a perfectly periodic fault as a first approximation to study the stability limit of a heterogeneous fault. We computed the eigenvalues of the static problem. They represent the limiting values of the weakening rate for which the modes are unstable. We showed the existence of a non-zero first eigenvalue for any geometry, that demonstrates the existence of a transition between stable and unstable behaviours. For any periodic fault, the threshold of instability is reached for a value of β (the weakening rate times the length of an individual fault) that is between two non-dimensional values associated with the limited cases of, first, infinitely distant faults and, secondly, infinitely narrow barriers. The first limiting value (1.157773...) was already computed for an isolated fault by Dascalu *et al.* (2000) and by Uenishi & Rice (2003). As a result of the non-dimensionality of β for an isolated fault, it is a universal threshold. A second universal limit emerges in our computation. When the barrier length tends to zero, the threshold is for $\beta = 0.153229....$ This non-zero limit means that, whatever is the weakening rate on the fault, it is sufficient to have a distribution of infinitely narrow barriers (i.e. with a surface that is asymptotically null) to keep the fault stable.

By drawing the analogy of our periodic problem with the infinite homogeneous case, we propose to interpret our results in terms of the effective friction on the homogenized fault (Campillo *et al.* 2001). We consider the global behaviour of a complex system and we search for the homogeneous system with a similar behaviour. Our analysis shows that the global behaviour of the periodic fault with slipping patches under a slip-weakening friction law can be either stable or unstable, depending on the geometry. In comparison with an infinite homogeneous fault, it means that the effective friction can be either weakening or strengthening.

Let us consider an actual fault in view of the results we obtained with the simplified periodic model. We focus our interest on the question of the growth of an instability that could be the initiation stage of a rupture at large scale. We found that the existence of segments under slip-weakening friction is not sufficient to imply the instability of the fault, even when the extension of the zone covered by such segments is very large and the surface of the barriers is very small. It illustrates the key importance of the small-scale structure of the fault. Even very limited geometrical irregularities can prevent the growth of the initiation. In this case, the fault can reach the stress threshold without developing a large-scale rupture. In this regime of stability, if a local stress concentration leads to a slip event, the further evolution is described by a solution with only propagative components. Formally this is the case when the dynamic eigenvalue problem has only solutions with negative squares. This results in the propagation of pulses that could be reflected by the barriers as it is illustrated in Dascalu *et al.* (2000). The effective behaviour is slip strengthening as observed in initial stage of the dynamic laboratory experiments (e.g. Ohnaka *et al.* 1987). In such a case, the quasi-static evolution of the fault is characterized by the concentration of stress at the edges of the barriers. Although our simplified model assumes unrealistic, infinitely resistant barriers, the evolution of a natural system, with barriers of finite resistance, includes

some form of barrier erosion. When the resistance threshold is exceeded, the slip may occur on a part of the barrier and the available length of the slipping patch is increasing. An increase in L (the half length of a slipping patch) results in an increase of β in the direction of the unstable domain. This suggests a scenario for the evolution of a heterogeneous fault in which two timescales are involved. The first timescale is related to the long-term evolution of the geometry with the erosion of the barriers as a result of stress concentration at their edges. The second is related to the onset of dynamic instability that is controlled by the effective weakening of the fault.

ACKNOWLEDGMENTS

The authors thank two anonymous reviewers and Raul Madariaga for their careful reading of the manuscript. The authors benefited from discussions with Hugo Perfettini, Christophe Voisin and Jean-Pierre Vilotte. This work was supported by the program ACI Prévention des Catastrophes Naturelles (Ministery of Research and Technology, France).

REFERENCES

Ampuero, J.-P., Vilotte, J.-P. & Sanchez-Sesma, F.J., 2002. Nucleation of rupture under slip dependent friction law: simple models of fault zone, *J. geophys. Res.,* **107**(B12), 10.1029/2001JB000452.

Andrews, D.J., 1985. Dynamic Plane-Strain Shear Rupture with a Slip-Weakening Friction Law Calculated by a Boundary Integral Method, *Bull. seism. Soc. Am.,* **75,** 1–21.

Aochi, H. & Fukuyama, E., 2002. Three-dimensional nonplanar simulation of the 1992 Landers earthquake, *J. geophys. Res.,* **107(B2),** doi:10.1029/2000JB00061.

Campillo, M. & Ionescu, I.R., 1997. Initiation of antiplane shear instability under slip dependent friction, *J. geophys. Res.,* **122**(B9), 20 363–20 371.

Campillo, M., Favreau, P., Ionescu, I.R. & Voisin, C., 2001. On the effective friction law of a heterogeneous fault, *J. geophys. Res.,* **106**(B8), 16 307–16 322.

Dascalu, C., Ionescu, I.R. & Campillo, M., 2000. Fault finiteness and initiation of dynamic shear instability, *Earth planet. Sci. Lett.,* **177,** 163–176.

Dieterich, J.H., 1986. A model for the nucleation of earthquake slip, in, *Earthquake Source Mechanics*, Vol. 37, pp. 37–47, eds Das, S., Boatwright, J. & Scholz, C.H., Geophys. Monogr. Ser., AGU, Washington, DC.

Guatteri, M., Spudich, P. & Beroza, G.C., 2001. Inferring rate and state friction parameters from a rupture model of the 1995 Hyogo-ken Nanbu (Kobe) Japan earthquake, *J. geophys. Res.,* **106,** 26 511–26 521.

Ida, Y., 1972. Cohesive force along the tip of a longitudinal shear crack and Griffith's specific surface energy, *J. geophys. Res.,* **77,** 3797–3805.

Ide, S. & Takeo, M., 1997. Determination of constitutive relations of fault slip based on seismic wave analysis, *J. geophys. Res.,* **102,** 27 379–27 391.

Ionescu, I.R. & Wolf, S., 2004. Interaction of faults under slip dependent friction. Nonlinear eigenvalue analysis, to appear in *Mathematical Methods in the Applied Sciences (M2AS)*.

Ionescu, I.R., Dascalu, C. & Campillo, M., 2002. Slip weakening friction on a periodic system of faults: spectral analysis, *Zeitschrift für angewandte Mathematik und Physik,* **53,** 1–17.

Knopoff, L., Landoni, J.A. & Abinante, M.S., 2000. The causality constraint for fractures with linear slip-weakening, *J. geophys. Res.,* **105,** 28 035–28 044.

Matsu'ura M., Kataoka, H. & Shibazaki, B., 1992. Slip Dependent Friction Law and Nucleation Processes in Earthquake Rupture, *Tectonophysics,* **211,** 135–148.

Ohnaka, M., 1996. Nonuniformity of the constitutive law parameters for shear rupture and quasistatic nucleation to dynamic rupture: A physical model of earthquake generation model. In: *Proc. Nat. Acad. Sci. USA. Earthquake Prediction: The Scientific Challenge,* Vol. 93, 3795–3802, Nat. Acad. Sci. USA, Irvine, CA.

Ohnaka, M., Kuwahara, Y. & Yamamoto, K., 1987. Constitutive relations between dynamic physical parameters near a tip of the propagating slip zone during stick-slip shear failure, *Tectonophysics,* **144,** 109–125.

Palmer, A.C. & Rice, J.R., 1973. The growth of slip surfaces in the progressive failure of overconsolidated clay slopes, *Proc. R. Soc. Lond.,* A, **332,** 527–548.

Papageorgiou, A.S. & Aki, K., 1983a. A specific barrier model for the quantitative description of inhomogeneous faulting and the prediction of strong ground motion Part I. Description of the model, *Bull. seism. Soc. Am.,* **73,** 693–722.

Papageorgiou, A.S. & Aki, K., 1983b. A specific barrier model for the quantitative description of inhomogeneous faulting and the prediction of strong ground motion Part II. Applications of the model, *Bull. seism. Soc. Am.,* **73,** 953–978.

Perfettini, H., Campillo, M. & Ionescu, I.R., 2003. On the rescaling of the slip weakening rate of heterogeneous faults, *J. geophys. Res.,* **108**(B9), 2410, doi:10.1029/2002JB001969.

Peyrat, S., Olsen, K. & Madariaga, R., 2001. Dynamic modelling of the 1992 Landers earthquake, *J. geophys. Res.,* **106,** 26 467–26 482.

Ruina, A.L., 1983. Slip instability and state variable friction laws, *J. geophys. Res.,* **88,** 10 359–10 370.

Uenishi, K. & Rice, J.R., 2003. Universal nucleation length for slip-weakening rupture instability under non-uniform fault loading, *J. geophys. Res.,* **108**(B1), ESE 17-1–17-14, cn:2042, doi:10.1029/2001JB001681, pp. .

Voisin, C., Ionescu, I.R., Campillo, M., Hassani, R. & Nguyen, Q.L., 2002. Initiation process on a finite segmented fault: a spectral approach, *Geophys. J. Int.,* **148,** 120–131.

Wolf, S., Manighetti, I., Campillo, M. & Ionescu, I.R., 2004. Mechanics of normal fault networks subject to slip weakening friction, *Geophys. J. Int.,* submitted.

APPENDIX A: INTEGRAL REPRESENTATION AND NUMERICAL APPROACH

For the convenience of the reader, we recall here from Ionescu *et al.* (2002) the principal steps of the solution technique used in solving the periodic eigenvalue problem. We first reduce the eigenproblem to a system of hypersingular integral equations and then we use an appropriate semi-analytic method to find solutions of period T.

Consider N arbitrary faults and denote by F their reunion. We suppose that $F \subset [0, T]$, $T > 0$, with $F = \cup_{i=1}^{N}[a_i, b_i]$ and that we have an infinite set of faults Γ_f, in which the geometry of the finite system F is repeated periodically. Namely,

$$\Gamma_f = \cup_{k\in\mathbb{Z}} F_k, \quad F_k = \cup_{i=1}^{N}[a_i + kT, b_i + kT]. \tag{A1}$$

The eigenproblem consists of finding φ: $R \times R_+ \to R$ and β such that

$$\nabla^2\varphi(x, y) = 0 \quad y > 0, \tag{A2}$$

$$\varphi(x, 0) = 0, \quad x \notin \Gamma_f, \tag{A3}$$

$$\frac{\partial\varphi}{\partial y}(x, 0) = -\beta\varphi(x, 0), \quad x \in \Gamma_f, \tag{A4}$$

$$\varphi(x + T, y) = \varphi(x, y). \tag{A5}$$

The Fourier transform in x of the eq. (A2) leads to

$$\varphi(x, y) = \frac{y}{\pi}\int_{\Gamma_f} \frac{\varphi(s, 0)}{y^2 + (s - x)^2} ds, \tag{A6}$$

which is a representation formula for the displacement field $\varphi\,(x, y)$. By derivation with respect to y and after some computations we deduce

$$\beta\varphi(x, 0) = -\frac{\pi}{T^2} FP \int_F \frac{\varphi(u, 0)}{\sin^2\left(\frac{\pi}{T}(x - u)\right)} du \tag{A7}$$

for $x \in F$, where the integral is taken in the finite-part sense. This equation is suitable for a numerical integration. For an efficient solving, we further look for a particular development of the spectral solution that takes into account the boundary conditions at the faults endpoints. Introducing $\varphi_i : [a_i, b_i] \to \mathbb{R}$ and the function $g : \mathbb{R} \to \mathbb{R}$ through

$$\varphi_i(t) = \varphi\left(\frac{b_i - a_i}{2} t + \frac{a_i + b_i}{2}, 0\right), \tag{A8}$$

$$g(z) = \begin{cases} 1/\sin^2(z) - 1/z^2 & \text{for } z \neq 0 \\ 1/3 & \text{for } z = 0 \end{cases} \tag{A9}$$

and the transformation variables s and t:

$$x = t\frac{b_k - a_k}{2} + \frac{a_k + b_k}{2} \quad u = s\frac{b_i - a_i}{2} + \frac{a_i + b_i}{2} \tag{A10}$$

we can write eq. (A7) as the following system of integral equations

$$\beta\varphi_k(t) = -\frac{2}{\pi(b_k - a_k)} FP \int_{-1}^{1} \frac{\varphi_k(s)}{(s - t)^2} ds - \frac{\pi}{T^2} \sum_{i=1}^{N} \int_{-1}^{1} H_{ik}(t, s)\varphi_i(s)\, ds \tag{A11}$$

for $t \in (-1, 1)$ and where

$$H_{ik}(t, s) = \frac{b_k - a_k}{2} g\left[\frac{\pi(s - t)}{T}\frac{b_k - a_k}{2}\right]\delta_{ik} + \frac{b_i - a_i}{2}\csc^2\left[\frac{\pi}{T}\left(t\frac{b_k - a_k}{2} + \frac{b_k + a_k}{2} - s\frac{b_i - a_i}{2} - \frac{b_i + a_i}{2}\right)\right](1 - \delta_{ik}). \tag{A12}$$

We look for the solution of this system in the form of the expansion

$$\varphi_k(t) = \sum_{n=1}^{\infty} U_{nk} \sin[n \arccos(t)] \tag{A13}$$

on $[-1, 1]$. With these notations the system of integral equations can be written in a compact form:

$$\beta\frac{b_k - a_k}{2} \sum_{n=1}^{\infty} A_{pn} U_{nk} = \sum_{i=1}^{N}\sum_{n=1}^{\infty} D_{pn}^{ki} U_{ni}, \tag{A14}$$

with

$$A_{mn} = -\frac{2mn[1 + (-1)^{m+n}]}{[(m - n)^2 - 1][(m + n)^2 - 1]}(1 - \delta_{n,m-1})(1 - \delta_{n,m+1}), \tag{A15}$$

$$B_{mn} = \frac{n\pi}{2}\delta_{m,n}, \tag{A16}$$

$$C_{pn}^{ki} = -\int_0^{\pi}\int_0^{\pi} \sin(n\psi)\sin(p\theta)\sin\psi\,\sin\theta\, H_{ik}(\cos\theta, \cos\psi)\, d\psi\, d\theta, \tag{A17}$$

$$D_{pn}^{ki} \equiv \begin{cases} \frac{b_k - a_k}{2}\frac{\pi}{T^2} C_{pn}^{ki} + B_{pn} & \text{for } i = k \\ \frac{b_k - a_k}{2}\frac{\pi}{T^2} C_{pn}^{kk} & \text{for } i \neq k. \end{cases} \tag{A18}$$

The relation in eq. (A14) is a generalized eigenvalue problem. In order to compute the corresponding matrices, we shall truncate the infinite series up to M. The eigenvalue form appears more clearly by defining the $NM \times NM$ matrices

$$\mathcal{A}_{lr} = \frac{b_k - a_k}{2} A_{pn}\delta_{i,k}; \quad \mathcal{D}_{lr} = D_{pn}^{ki}, \tag{A19}$$

with $l = M \times (k-1) + p$ and $r = M \times (i-1) + n$ for $p, n = \overline{1, M}$ and $i, k = \overline{1, N}$. Also the generalized eigenvectors

$$v_r = U_{ni}, \tag{A20}$$

for $r = M \times (i-1) + n$ with $n = \overline{1, M}$ and $i = \overline{1, N}$.

With eqs (A19) and (A20) the system in eq. (A14) now reduces to the generalized eigenproblem

$$\beta \sum_{q=1}^{NM} \mathcal{A}_{lq} v_q = \sum_{q=1}^{NM} \mathcal{D}_{lq} v_q, \tag{A21}$$

for the eigenvalue β and the eigenvectors v.

APPENDIX B: STRUCTURE OF THE SPECTRUM

The structure of the spectrum of the solution is governed by the existence of a series of eigenvalues α_n^1 corresponding to the elementary periodicity P of the system. For large n, we observe qualitatively, that the eigenfunction $\varphi_n^1(x, y) \approx \sin(n\pi x/(2L)) f(y)$ and from eq. (17) we deduce $f(y) = K \exp(-n\pi y/(2L))$ with K a constant. Replacing in eq. (19) we found that $\alpha_n^1 \approx n\pi/(2L)$ for large n. According to our numerical results, the interval between two eigenvalues is rapidly converging towards $\pi/2$ for increasing eigenvalue index (Fig. B1). As already stated, each of these eigenvalues is also a solution for any periodicity multiple of P.

When plotting the eigenvalues for all periodicity mP (Fig. B2), we notice that the eigenvalues for period mP are concentrated closely around the solution for the elementary period P. This phenomenon can be regarded as a progressive splitting of the solution of elementary period. There is m eigenvalues around α_n^1 for solutions of periodicity mP. We noted that this split eigenvalue is larger than α_n^1 when n is odd and is smaller when n is even. In other words, noting that $\alpha_{nm-1}^m = \alpha_n^1$ we remark that $\alpha_{nm}^m > \alpha_n^1$ when n is odd and $\alpha_{nm}^m < \alpha_n^1$ when n is even. All the eigenvalues degenerated from α_n^1 lie between α_n^1 and α_{2n}^2. Accordingly we can define for every α_n^1 a splitting width and we found numerically that this width is decreasing with n faster than n^{-2}. It must be noted that the eigenvalues lying strictly inside this interval (i.e. the eigenvalues different from the limits of the splitting interval) are twice degenerated. For example, let us consider the first eigenvalue. For $m = 2$ we found two split eigenvalues that define the splitting domain, one of them being α_0. For $m = 3$, we found three eigenvalues: α_0 and two identical values. Three modes are nevertheless present because the degenerate values correspond to two distinct eigenfunctions.

In order to interpret the repartition of the eigenvalues, we present in Fig. B3 the eigenfunctions along the fault, that is the distribution of slip. We show only the eigenfunctions associated with the first three groups of eigenvalues and for the three first periodicities. The plots are presented in the same order as the eigenvalues in Fig. B2. We did not repeat the eigenfunctions of elementary periodicity, which are trivially solutions for every periodicities. Note that for $m = 3$, we observe couples of eigenfunctions that are different but each couple is associated with a single eigenvalue. The shapes of the displacement distributions (Fig. B3) help to understand why the first eigenvalues split from α_0 by larger values. For example, the solution of period $2P$ ($n = 1$, $m = 2$) exhibits a pattern such that two neighboring patches slip in opposite directions. This is indeed a less unstable situation than the one of the very first eigenvalue with all segments slipping in the same direction. An opposite case is encountered with the second mode of periodicity P. Its eigenfunction ($n = 1$, $m = 1$) shows that slip in opposite directions occurs on the elementary fault itself. For a larger periodicity, for example $m = 2$, the pattern of slip is such that two adjacent segments of faults interact with the closest zones of slip being in the same direction. This leads to a more unstable situation than for the one of the solution

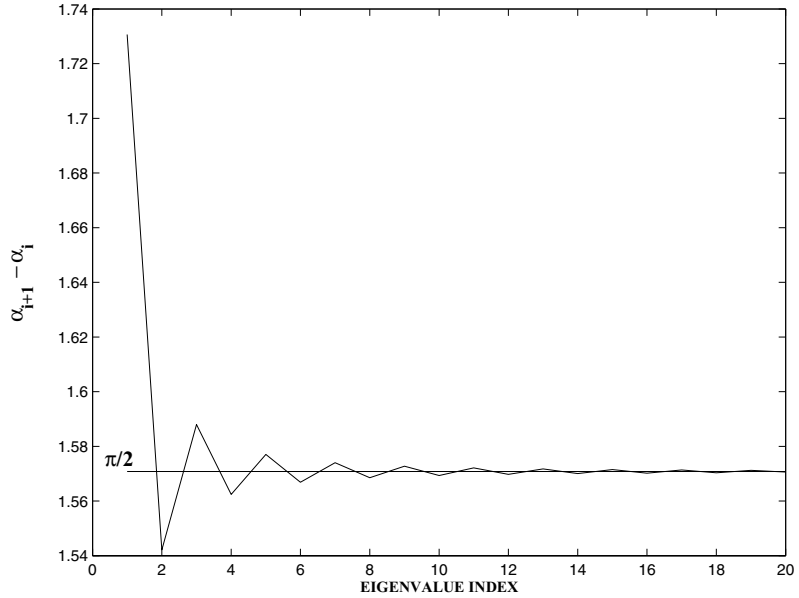

Figure B1. Difference between two successive eigenvalues $L(\alpha_{n+1}^1 - \alpha_{n)}^1$ for an elementary period ($m = 1$). Note the convergence to $\pi/2$ for large n.

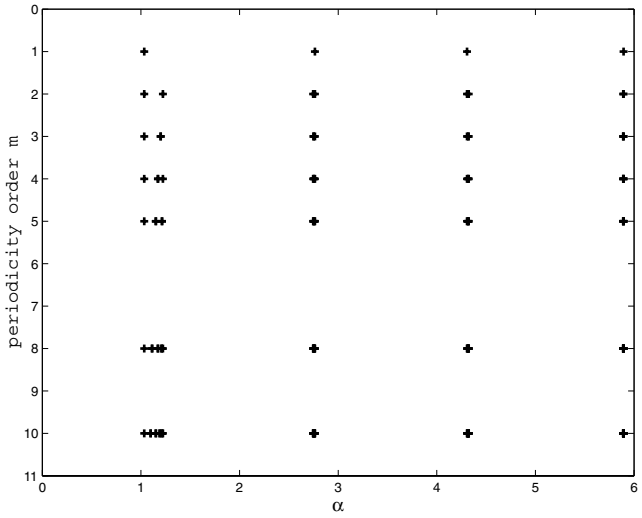

Figure B2. The eigenvalues α_n^m from different periodicity mL of the solution.

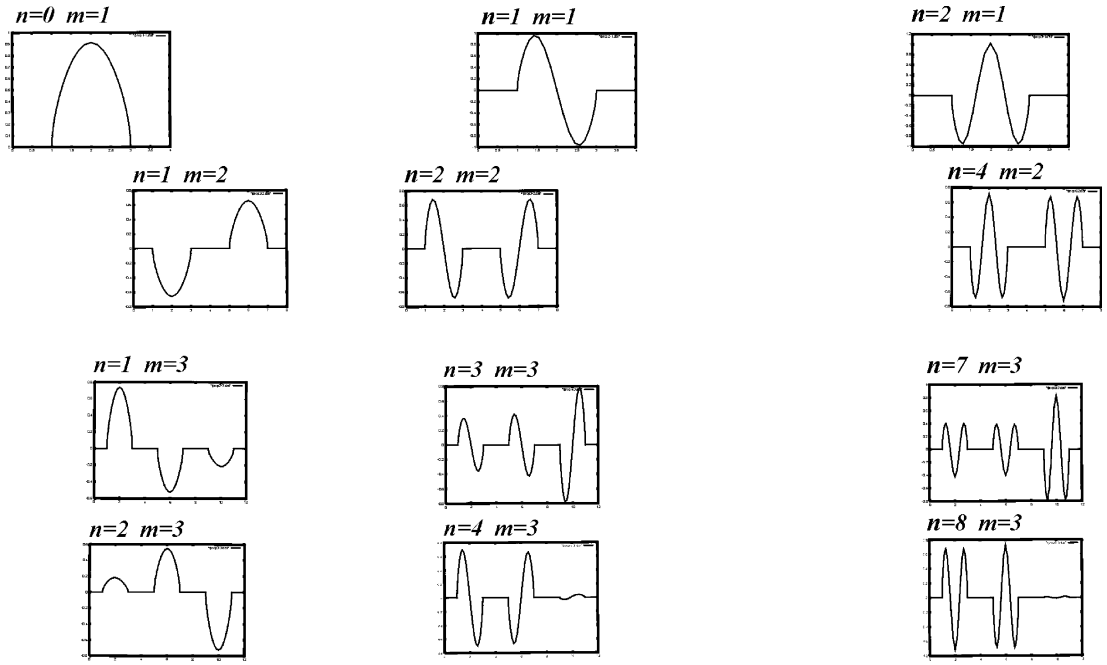

Figure B3. Shapes of the slip distribution associated with the eigenfunctions $\varphi_n^m(x, 0)$.

with the elementary periodicity P. As a consequence of these symmetry properties, the eigenvalues close to α_1^1 split by smaller values. Similar observations can be done for the other modes. An important conclusion, which can be drawn from this description of the spectrum, is that the stability limit of the entire periodic system is given by the first eigenvalue in the set of solutions having the elementary periodicity P. According to the previous analysis, the only exception would be that the first split eigenvalue of α_1^1 for periodicity $2P$, which is smaller than α_1^1, is also smaller than α_0. Such a case was not encountered in the computations we performed.